Hindawi
Advances in Condensed Matter Physics
Volume 2018, Article ID 2028491, 8 pages
https://doi.org/10.1155/2018/2028491

*Research Article*

# Ion Migration Polarization in the Yttria Stabilized Zirconia Based Metal-Oxide-Metal and Metal-Oxide-Semiconductor Stacks for Resistive Memory

**Stanislav Tikhov**[1], **Oleg Gorshkov**[2,3], **Ivan Antonov**[2], **Alexander Morozov**[1], **Maria Koryazhkina**[2] and **Dmitry Filatov**[3]

[1]*Department of Physics, Lobachevsky State University of Nizhny Novgorod, 23 Gagarin Ave., Nizhny Novgorod 603 950, Russia*
[2]*Research Institute for Physics and Technology, Lobachevsky State University of Nizhny Novgorod, 23 Gagarin Ave., Nizhny Novgorod 603 950, Russia*
[3]*Research and Educational Center for Physics of Solid State Nanostructures, Lobachevsky State University of Nizhny Novgorod, 23 Gagarin Ave., Nizhny Novgorod 603950, Russia*

Correspondence should be addressed to Dmitry Filatov; dmitry_filatov@inbox.ru

Received 4 November 2017; Revised 7 January 2018; Accepted 12 April 2018; Published 14 May 2018

Academic Editor: Sergei Sergeenkov



We report the investigations of the ion migration polarization in the yttria stabilized zirconia (YSZ) thin films in the Metal-Oxide-Metal (MOM) and Metal-Oxide-Semiconductor (MOS) stacks due to the drift of the oxygen vacancies under the external bias voltage applied between the electrodes. The parameters characterizing the drift of the oxygen vacancies in YSZ such as the ion drift activation energy, mobile ion concentration, and the drift mobility have been determined in the temperature range 300–500 K. These data are important for deeper understanding of the fundamental mechanisms of the electroforming and resistive switching in the YSZ-based MOM and MOS stacks, which are promising for the Resistive Random Access Memory (RRAM) and other memristor device applications.

## 1. Introduction

The phenomenon of resistive switching in thin dielectric films has attracted much attention in last decade [1]. This phenomenon consists in a reversible persistent change of the resistance of thin (several tens nanometers thick) dielectric films sandwiched between two conductive electrodes under the external bias voltage applied between the electrodes. The electron devices utilizing the resistance switching effects are called *memristors* [2]. The potential fields of application of the memristors include the development of the nonvolatile computer memory of new generation (Resistive Random Access Memory, RRAM) [3, 4], neuromorphic electron devices [5–7] and so on.

Today's understanding of the origin of the resistive switching in the metal oxides is based on the concept of the migration (the drift and/or diffusion) of the oxygen ions in the external electric field [8]. This process can be also described in terms of the migration of the charged oxygen vacancies. The oxygen vacancies in the electric fields between the electrodes of the memristor structure tend to arrange in the conductive filaments, which shortcut the electrodes (so-called forming process) [9]. As a result, the memristor switches from the initial high resistance state (HRS) to the low resistance state (LRS). The HRS can be restored by applying a voltage pulse of the opposite polarity destroying the filaments. Further operation of the memristor is provided by the restoring and rapture of the filaments resulting in switching the memristor from HRS to LRS and back (referred to as the SET process and the RESET one, resp.). It is obvious from the above that the oxygen ion transport plays a key role in the mechanism of resistive switching in the metal oxides. For deeper understanding of the resistive switching mechanism in these materials, it is important to know

the parameters of the oxygen ion transport, such as the activation energies for the oxygen ion migration, the mobile ion concentration, and mobility. Knowing these parameters is essential to find the ways to improve the performance (first of all—the reproducibility and the reliability) of the memristor devices based on the metal oxides.

Yttria stabilized zirconia (YSZ) $ZrO_2(Y)$ is a promising material for the memristor devices [10–13]. It is featured by a high concentration of oxygen vacancies that provides the high anion mobility [14]. It is clear from the above, that the availability of the oxygen vacancies is essential for the manifestation of resistive switching in the metal oxides since the oxygen ion transport in these materials goes through the jumps of the oxygen ions into the adjacent oxygen vacancy sites. Usually, the necessary oxygen vacancy concentration in the metal oxide films for the memristor devices is achieved either by deposition of the nonstoichiometric oxide films or by the postdeposition vacuum annealing. In contrary, in YSZ the necessary oxygen vacancy concentration is provided by doping by the stabilizing oxide $Y_2O_3$ [15]. This intrinsic property of YSZ opens a way to a precise control of the oxygen vacancy concentration by varying the molar fraction of $Y_2O_3$ (the vacancy concentration is 1/2 that of the Y atoms). To date, the prototype memristor devices based on the YSZ films have been fabricated and demonstrated a good durability (up to $10^7$ SET/RESET cycles) [12, 13].

In the present study, we have measured the oxygen ion transport parameters in the thin YSZ (≈12% mol. $Y_2O_3$) films deposited by Magnetron Sputtering by studying the ion migration polarization [16] in the Metal-Oxide-Metal (MOM) and Metal-Oxide-Semiconductor (MOS) stacks based on these films. Several methods have been applied to identify the polarization mechanism and to determine the ion transport parameters: measuring the capacitance-voltage (*C-V*) curves, the high-frequency (HF) conductivity (*G-V* curves), the depolarization current [17], and the quasistatic capacitance of the MOS and MOM stacks. Besides, a novel method based on measuring the temperature dependence of the hysteresis in the cyclic current-voltage (*I-V*) curves has been proposed in the present study. This method is a variant of the classical one of measuring the dynamic *I-V* curves [18].

## 2. Materials and Methods

The MOM stacks were deposited onto the Si substrates oxidized and covered by the Ti (25 nm thick) and TiN (25 nm thick) metallization layers. The MOS stacks were deposited on the *n*- and *p*-Si(001) substrates with the specific resistivity of 4.5 Ω·cm. The YSZ films were deposited at the substrate temperature $T_g = 300^\circ$C by Radio Frequency Magnetron Sputtering of the $ZrO_2$ + 12% $Y_2O_3$ target in the Ar-$O_2$ (50 : 50% mol.) gas mixture. The YSZ film thicknesses $d$ were 10, 15, and 40 nm. The Au gates of 40 nm in thickness with Zr or Ta sublayers were deposited onto the YSZ films at $T_g = 200^\circ$C through a shadow mask. The values of the sublayer thickness $d_s$ were 3, 5, and 15 nm; the ones of the gate area $S$ were $\approx 10^{-3}$ and $\approx 10^{-2}$ cm$^2$. To measure the temperature dependencies of the *C-V*, *G-V*, and the dynamic *I-V* curves, the samples were placed into a vacuum-pumped thermostat providing the variation of the sample temperature $T$ within the range 77–300 K. The measurements in the temperature range 300–510 K were performed in ambient air using either the isothermic regime or the rapid heating/cooling one. The uncertainty of the temperature measurements was ≈1°C.

The measurements of the *C-V*, *G-V*, and *I-V* curves were performed using Agilent® B1500A semiconductor device analyzer. The HF *C-V* and *G-V* curves were measured at the frequency $f = 100$ kHz with the ramp voltage sweep within the range −3–+3 V with a constant sweep rate $\beta$. The dynamic *I-V* curves were measured at several values of $\beta$ ranging from 0.002 to 0.02 V/s. The ranges of the ramp voltage sweep were 0-1 V and 0–2 V. These measurements were performed in the isothermic regime at the temperature $T$ varied within the range 300–510 K.

In order to measure the depolarization current, the samples have been heated up to 510 K under the polarizing voltage $V = 1.2$ V and then were quenched down by the immersion into a Dewar flask filled with liquid nitrogen in order to freeze the polarized state. Then the samples were heated up with the rate ≈0.4°C/s at $V = 0$, and the depolarization current was measured. The quasistatic capacitance and its temperature dependencies were studied by measuring the discharge current of the MOS and MOM stacks after the charging by a constant voltage ranging from 0.1 to 2 V. It should be stressed here that all measurements were performed avoiding the forming and resistive switching; that is, the measured oxygen ion transport parameters were the intrinsic ones of the as-deposited YSZ films.

## 3. Results and Discussion

Typical HF *C-V* and *G-V* curves for the MOS stack with the YSZ insulating layer and Zr underlying one measured at various temperatures are presented in Figure 1. The values of $G$ for the HF *G-V* curves were normalized to the circular measurement frequency $\omega = 2\pi f$. All measurement results are given for the gate area $S = 10^{-2}$ cm$^2$; the positive values of the bias voltage $V$ correspond to the positive potential at the metal gates with respect to the substrates. An anomalous hysteresis was observed in the *C-V* and *G-V* curves at $T > 300$ K. This kind of hysteresis can be attributed to the ion migration in YSZ [19], whereas the normal hysteresis typical for the *C-V* and *G-V* curves of the MOS stacks originates from the exchange by electrons or holes between the semiconductor substrate and the surface states at the semiconductor/insulator interface [18].

The values of area within the hysteresis loops increased with increasing temperature in the temperature range 350–400 K. At higher temperatures, the hysteresis loop width tended to saturate and even decreased with increasing temperature. The *C-V* and *G-V* curves with such behavior of the temperature dependence of the hysteresis loop width were observed in the MOS stacks with relatively low density of surface states at the YSZ/Si interfaces. The values of the surface state density were obtained from the frequency and temperature dependencies of the admittance of the MOS

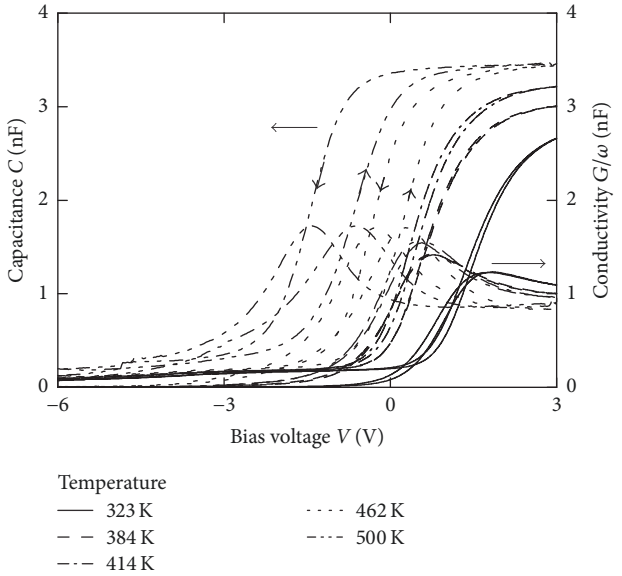


Figure 1: *C-V* and *G-V* curves of the Au/Zr (3 nm)/YSZ (40 nm)/*n*-Si MOS stack measured at various temperatures. Ramp voltage sweep rate $\beta = 0.04$ V/s, measurement frequency $f = 100$ kHz.

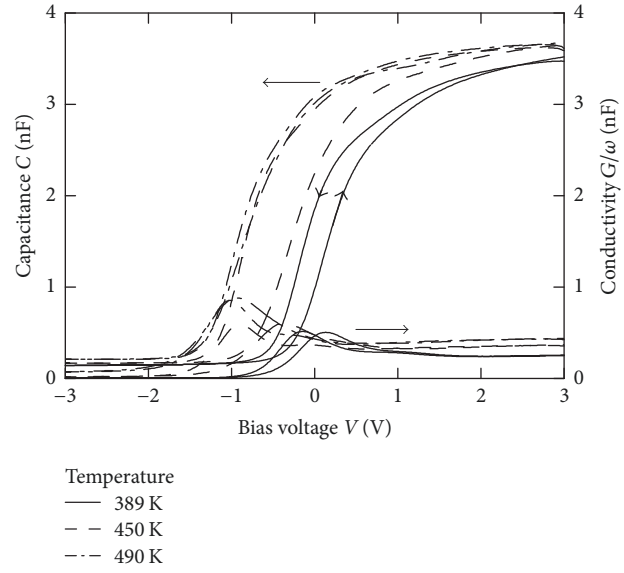


Figure 2: *C-V* and *G-V* cures of Au/Ta (5 nm)/YSZ (40 nm)/*n*-Si MOS stack measured at various temperatures. Ramp voltage sweep rate $\beta = 0.04$ V/s, measurement frequency $f = 100$ kHz.

stacks using the model of single level surface states [20]. The ionization energy $E_i \approx 0.47$ eV and the density of the surface states $N_s \approx 4.7 \cdot 10^{11}$ cm$^{-2}$ were found. The specific density of the surface states $N_{ss}$ at $V = V_{FB}$ ($V_{FB}$ is the flat band voltage) was estimated using the differential method [20] to be $<5 \cdot 10^{11}$ cm$^{-2}$·eV$^{-1}$.

In the samples with the Ta sublayers, the values of $N_{ss}$ were higher than in the samples with the Zr ones ($\approx 4 \cdot 10^{12}$ cm$^{-2}$·eV$^{-1}$). The anomalous hysteresis in the *C-V* and *G-V* curves disappeared completely at higher temperatures (Figure 2). This result confirms the conclusion drawn above that the decrease of the anomalous hysteresis in the *C-V* and *G-V* curves of the YSZ-based MOS stacks with increasing temperature originated from the recharging of the surface states at the YSZ/Si interface.

Figure 3 presents the temperature dependencies of the flat band voltage shift $\Delta V_{FB}$ at the flat band capacitance level $C_{FB}$ in the anomalous hysteresis loops of the MOS stacks with different $N_{ss}$. For all MOS stacks with relatively low $N_{ss}$, the temperature intervals of growing $\Delta V_{FB}$ with increasing temperature were observed. Within these intervals, the temperature dependencies of $\Delta V_{FB}$ obeyed Arrhenius law with the activation energy $E_a \approx 0.5$ eV (Figure 3, curves *(1)* and *(2)*).

At higher temperatures, the saturation and even some decay of $\Delta V_{FB}$ with increasing temperature was observed. Within this temperature interval, the highest concentration of the mobile ions responsible for the anomalous hysteresis was reached. The reduced surface density of the mobile ions $N_{Is}$ could be estimated using the following formula [20]:

$$N_{Is} = \frac{C_D \Delta V_{FB}}{eS}, \quad (1)$$

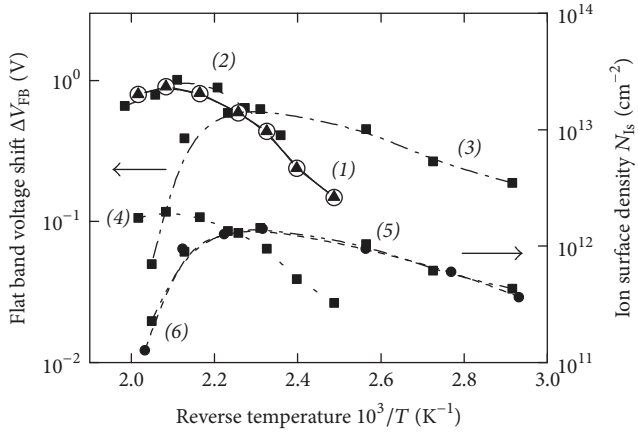


Figure 3: Temperature dependencies of the frat band voltage shift $\Delta V_{FB}$ *(1–3)* and the ones of the reduced mobile ion density $N_I$ *(5, 6)* for the MOS stacks with different values of $N_{ss}$, cm$^{-2}$·eV$^{-1}$: *(1, 2, 4)*—$5 \cdot 10^{11}$; *(3, 5)*—$4 \cdot 10^{12}$. Substrate: *(1, 3–5)*—*n*-Si, *(2)*—*p*-Si.

where $C_D$ is the capacitance of the insulator determined from the saturated capacitance in the *C-V* curves (Figures 1 and 2) and $e$ is the elementary charge. As follows from (1), $N_{Is}$ is proportional to $\Delta V_{FB}$. As the temperature dependence of $\Delta V_{FB}$ obeys Arrhenius law in certain temperature range, the same should hold for $N_{Is}$. The origin of such temperature dependence of $N_{Is}$ is the activation nature of the ion conductivity in YSZ as well as in other solid electrolytes [15].

The value of $N_s$ determined from curve *(4)* in Figure 3 was $\approx 2 \cdot 10^{12}$ cm$^{-2}$. Assuming the mobile ions to be distributed uniformly inside the YSZ film with the thickness $d \approx 40$ nm, the mobile ion concentration $N_I$ can be estimated as $N_I = N_{Is}/d \approx 5 \cdot 10^{17}$ cm$^{-3}$. This value is an underestimate obviously since typical value of the oxygen vacancy concentration in

single crystal YSZ is ~$10^{21}$ $cm^{-3}$ [21]. This disagreement could be attributed to a nonuniform distribution of the electric field inside the YSZ film. Indeed, once the oxygen vacancies are charged positively, the maximum electric field strength should take place at the YSZ/gate interfaces. It may seem reasonable to assume that the ion drift takes place primarily in these thin YSZ layers adjacent to the metal gates, and the remaining volume of the YSZ film does not contribute into the ion transport. However, this hypothesis cannot explain too low values of $N_I$ obtained for the MOS stacks. If it were true, the thickness of the layer containing the mobile ions could be estimated as ~$10^{-4}d \sim 10^{-3}$ nm for $d = 40$ nm. This value is much less than the lattice constant of YSZ (≈0.63 nm).

The underestimate of $N_I$ obtained from the anomalous hysteresis in the *C-V* curves of the MOS stacks was attributed to the simultaneous coexistence of the electron transport (the recharging of the surface states) along with the oxygen ion transport in YSZ. Both effects result in the hysteresis in the *C-V* and *G-V* curves. However, the contributions of these two effects into the resulting values of $\Delta V_{FB}$ have the opposite signs, and these ones compensate each other. The effect of compensation is more pronounced at higher temperatures because the higher the temperature, the more the impact of the surface states on the hysteresis in the *C-V* and *G-V* curves. Also, the impact of the surface states should increase with increasing $N_{ss}$. This effect was observed in the experiment indeed (cf. Figures 1 and 2) which confirms the explanation given above.

In order to obtain more reliable data on the mobile oxygen ion concentration $N_I$ in the YSZ films under study, we performed the investigations of the ion migration polarization in the MOM stacks based on these films. It is well known that studying the ion transport in the dielectrics meets a number of problems often (the difficulty to find out the relation of the electric current in the external circuit to the ion transport inside the insulator, the electrochemical phenomena at the electrodes, etc. [22]). Therefore, we have applied a number of alternative measurement methods. Typical dynamic *I-V* curves of an YSZ-based MOM stack measured at various temperatures are presented in Figure 4. The dynamic *I-V* curves did not depend on the polarity of the bias voltage $V$. The direction of the hysteresis loop was always the same (as shown in Figure 4).

The hysteresis observed in the dynamic *I-V* curves could be attributed either to the ion migration polarization of the insulator or to a trap one. After sweeping the bias voltage $V$ from 0 V up to its maximum value and back down to 0 V, a nonzero negative residual current $\Delta I_{res}$ was observed at $V = 0$. So far, the observed hysteresis in the dynamic *I-V* curves can be attributed to the electret effect [23, 24]. The magnitude of the effect increased with increasing temperature. It should be noted that the electret effect was most pronounced in the same temperature range, where the ion polarization-related anomalous hysteresis was manifested in the *C-V* and *G-V* curves of the YSZ-based MOS stacks (cf. Figures 1, 2, and 4). So far, the hysteresis observed in the dynamic *I-V* curves of the YSZ film-based MOM stacks can be related to the inertia of the oxygen ion drift when increasing and decreasing

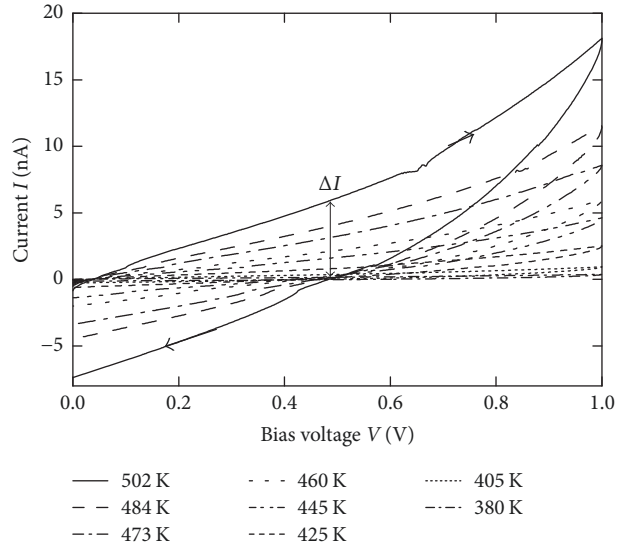


Figure 4: Dynamic *I-V* curves of the Au/Zr (3 nm)/YSZ (40 nm)/TiN MOM stack measured at various temperatures. Ramp voltage sweep rate $\beta = 0.02$ V/s.

the bias voltage $V$. Namely, the ion transport in the YSZ films can affect the electric field strength distribution inside these ones, which, in turn, results in the transient electric currents in the external electric circuit reflecting the ion drift inside the YSZ films. The hysteresis loop related to the ion migration polarization in the higher temperature range did not depend on the ramp voltage sweep rate $\beta$ (varied from 0.002 up to 0.02 V/s). So far, one can exclude the effect of the displacement current. The charging and discharging of the MOM capacitors cannot take effect as well since typical time constant of the current relaxation was $<10^{-6}$ s as determined from the measurements of the small signal parameters of the equivalent scheme.

Since the magnitude of the hysteresis loop did not depend on the sign of the bias voltage $V$ applied to the metal electrodes at given measurement temperature, one can conclude the charges of the ions and traps in the investigated samples to be distributed uniformly within the YSZ film before the polarization [23]. The net charge $\Delta Q$ can be determined from the area of the hysteresis loop using the following relation [18]:

$$\Delta Q = \frac{1}{\beta}\left(\int_0^V I\,dV - \int_V^0 I\,dV\right). \quad (2)$$

Figure 5 presents the temperature dependencies of $\Delta Q$ (curves *(1)* and *(2)*), of the forward current at zero reverse one (see Figure 4 for explanation) $\Delta I$ (curve *(3)*), and of the residual current $\Delta I_{res}$ (curve *(4)*). These temperature dependencies can be approximated by the combinations of two straight lines in the Arrhenius axes with the activation energies ≈0.55 eV (at $T > 380$ K) and ≈0.2 eV (at $T < 380$ K). The former activation energy can be related to the activation of the ion transport. This process was also manifested in the MOS stacks with relatively low density of surface states as well as in the MOM ones with the YSZ layers of various thickness

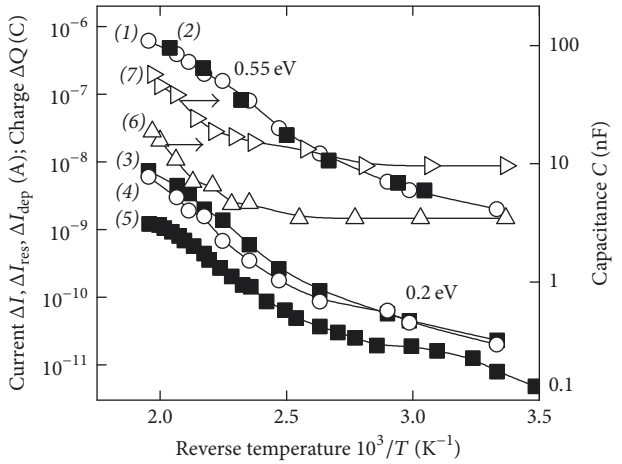


FIGURE 5: Temperature dependencies of the net charge $\Delta Q$ *(1, 2)*, of the forward current at zero reverse one $\Delta I$ *(3)*, of the residual current $\Delta I_{res}$ *(4)*, of the depolarization current $I_{dep}$ *(5)*, and of the quasistatic capacitance *(6, 7)* of the MOM stacks with different YSZ film thicknesses $d$, nm: *(1)*—15; *(2–6)*—40, *(7)*—10.

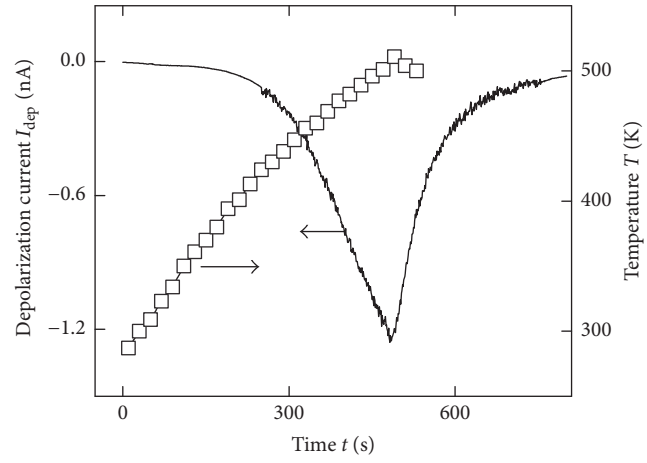


FIGURE 6: Kinetics of the temperature $T$ and the depolarization current $I_{dep}$ for the MOM stack based on the YSZ film with $d$ = 40 nm.

(15 nm and 40 nm) regardless to the gate sublayer material (Zr or Ta). The latter activation process can be related to the traps in YSZ. This effect was observed in the YSZ films deposited by Magnetron Sputtering only and was not observed in single crystal YSZ [25].

Assuming the uniform distribution of the charge in the YSZ films before the polarization, the surface density of the charge $N$ was estimated according to the formula

$$N = \frac{\Delta Q}{eS}. \tag{3}$$

The values of the reduced surface concentration of the mobile ions in the YSZ films $N_{Is}$ obtained from the dynamic *I-V* curves of the MOS stacks were not saturated with increasing temperature (unlike the ones obtained from the *C-V* curves of the MOS stacks) and can be estimated as $\approx 5 \cdot 10^{14}$ cm$^{-2}$ at $T \approx 505$ K. Correspondingly, the reduced surface density of the traps in the films of ≈40 nm in thickness was estimated to be $\approx 1.2 \cdot 10^{12}$ cm$^{-2}$. On the other hand, as it has been already mentioned above, the volume concentration of the oxygen vacancies in the single crystal YSZ with 12% mol. of $Y_2O_3$ is $\sim 10^{21}$ cm$^{-3}$ which corresponds to the surface vacancy concentration of $\sim 10^{14}$ cm$^{-2}$. So far, the oxygen vacancies in the investigated YSZ films were concentrated in a layer at least 5 times thinner than the YSZ film itself.

Also, the temperature dependencies of the quasistatic capacitance $C$ of the MOM stacks with the YSZ film thicknesses $d \approx 40$ nm (curve *(6)*) and ≈10 nm (curve *(7)*) are presented in Figure 5. These data support the estimates of the activation energies given above. Starting from $T \approx 380$ K corresponding to the beginning of manifestation of the ion migration polarization, the values of $C$ begin to grow with increasing temperature for all values of $d$. At higher temperatures, this growth obeyed Arrhenius law with the activation energies ranging from 0.50 to 0.53 eV. These values are close to the ones for the ion migration obtained from the measurement of the *C-V* curves of the MOS stacks and of the dynamic *I-V* curves of the MOM ones. Assuming the dielectric permittivity of YSZ to be constant, one can estimate the thickness of the conductive layer in the YSZ film from the capacitance ratio at the maximum capacitance and temperature as ≈1.6 nm for $d = 10$ nm and ≈6.9 nm for $d = 40$ nm. At the same time, the quasistatic capacitance was not saturated with increasing temperature. This fact points to an incomplete ion polarization. The nonlinear electrical properties of the YSZ-based MOS and MOM stacks evidence the presence of the ions in the insulating layers, which become mobile in strong enough electric field (~$10^5$ V/cm) at higher temperatures and concentrated in a thin space charge layers adjacent to the metal gates.

Typical kinetics of $T$ and of $I_{dep}$ after the polarization of the MOM stack with the YSZ film thickness $d = 40$ nm are presented in Figure 6. The sample was polarized at constant $V = 1$ V and $T = 510$ K and was cooled down to 300 K rapidly. Then the sample was heated up again at $V = 0$. The maximum absolute value of $I_{dep}$ took place near $T = 500$ K. The analysis of the depolarization curve has shown the temperature dependence of $I_{dep}$ to obey Arrhenius law when increasing $T$. The activation energy was ≈0.55 eV. This value is close to the ones obtained from the *C-V* measurements of the MOS stacks as well as from the measurements of the dynamic *I-V* curves and of the quasistatic capacitance of the MOM stacks. One can determine the charge of the polarizing ions from the area under the depolarization curve:

$$\Delta Q = \int_0^t I\, dt. \tag{4}$$

The resulting values almost match the ones determined from the dynamic *I-V* curves. The activation energy of the ion conductivity for the oxygen vacancies in single crystal zirconia stabilized in the cubic phase is known to fall into the range 1.0–1.2 eV [14, 21]. As it has been shown in [14], this activation energy consists of two nearly equal components: (i) the energy of detachment of the ion from the lattice and (ii)

the energy of its further motion over the potential barriers as it takes place in the classic mechanism of the ion migration polarization [23]. In the samples studied in the present work, the activation energies scattered from 0.5 to 0.6 eV. This could probably be related to the polycrystalline (nanocrystalline) structure of the investigated YSZ films so that the oxygen ions can move along the grain boundaries [26, 27]. Earlier, High Resolution Transmission Electron Microscopy studies demonstrated the YSZ films in the investigated stacks to have a nanocrystalline structure with the average grain sizes ≈40 nm (in the 40 nm thick YSZ films); the grain boundaries were perpendicular to the substrate [12]. The theory of the ion transport along the grain boundaries is absent to date. Probably, the activation energy of the ion transport along the grain boundaries is less than the one for the ion transport in single crystals [26].

One can estimate the ion mobility from the dynamic *I-V* curves presented in Figure 4. Assuming a uniform distribution of the ions in the YSZ films before the polarization, one gets

$$N_{\mathrm{I}} = \frac{\Delta Q}{edS}. \tag{5}$$

The film conductivity $G$ can be estimated from the slope of the linear parts of the reverse branches of the dynamic *I-V* curves shown in Figure 4 (when sweeping $V$ back from 1 V down to 0 V). This implies that if the polarization originates from the ion migration in the insulator, then the variation of the electric current in the external circuit equals the one of the ion current, that is, the oxygen vacancies arrive at the cathode and contribute to the electric current in the external circuit, but do not capture the electrons. In this case, one can estimate the ion mobility from the following relations for the ion conductivity $\sigma_{\mathrm{I}}$:

$$\sigma_{\mathrm{I}} = G\frac{d}{S}, \tag{6a}$$

$$\sigma_{\mathrm{I}} = e\mu N_{\mathrm{I}}. \tag{6b}$$

Let us assume the concentration of the mobile ions $N_{\mathrm{I}} \sim 10^{20}\,\mathrm{cm}^{-3}$ to be constant, and the number of the polarized ions to grow with increasing temperature because of the increasing of the probability of the ion jumps over the potential barrier.

The temperature dependencies of $\sigma_{\mathrm{I}}$ and $\mu$ are presented in Figure 7. The values of $\mu$ increase with increasing temperature from $4.3\cdot10^{-14}$ cm$^2$/V·s at 425 K up to $2.8\cdot10^{-13}$ cm$^2$/V·s at 502 K. This result can be considered as an evidence of the polarization mechanism related to increasing the ion mobility with increasing temperature. In turn, this fact evidences the barrier mechanism of the ion transport in the YSZ films [14, 28]. The increase of the ion mobility with increasing temperature obeys Arrhenius law with the activation energy ranging from 0.50 to 0.55 eV corresponding to the height of the potential barrier between the ions. This value coincides with the ones obtained in the present study from the dynamic *I-V* curves, from the depolarization current measurements, and from the quasistatic capacitance of the MOM stacks as well as from the *C-V* measurements of the MOS stacks.

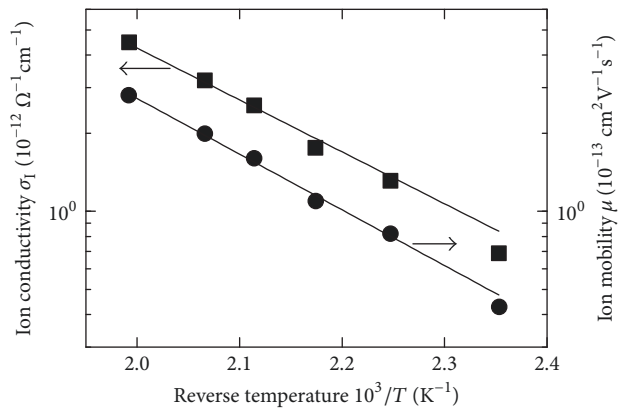


Figure 7: Temperature dependencies of the ion conductivity $\sigma_{\mathrm{I}}$ and ion mobility $\mu$ in the YSZ films.

Also, one can estimate the drift mobility of the ions $\mu$ from the time-of-flight of the ions between the electrodes of the MOM stacks $\tau$ determined from the kinetics of charging due to the ion migration polarization when applying a bias voltage between the electrodes [17]. Assuming the absence of diffusion as well as of the electrochemical reactions at the electrodes (so that the ion transport is characterized by the ion drift mobility only) [29, 30], in the case of normal (Gaussian) transport one has

$$\tau = \frac{d}{\mu F}. \tag{7}$$

That is, $\tau$ is proportional to the $d/F$ ratio where $F$ is the electric field strength in the insulator. This estimate gives the value of ion mobility $\mu \approx 4\cdot10^{-13}$ cm$^2$/V·s at 500 K. This value is close to the one obtained from the dynamic *I-V* curves in spite of neglecting the phenomena at the electrodes as well as the electrostatic interaction between the ions, which may be essential at high ion concentrations in the investigated YSZ films (~$10^{19}$–$10^{20}$ cm$^{-3}$). The parameters of the oxygen ion transport in the YSZ films of different thicknesses $d$ determined for various materials and thicknesses of the sublayers under the Au gates $d_{\mathrm{s}}$ by various methods are summarized in Table 1.

As follows from Table 1, the parameters of the ion transport in the MOS and MOM stacks measured by various methods did not depend on the materials and thicknesses of the gate sublayers. Also, it follows from Table 1 that the *C-V* measurements of the MOS stacks gave too low values of the mobile ion concentration $N_{\mathrm{I}}$ as compared to the ones obtained by other methods. As it has been already pointed out above, this discrepancy could be ascribed to the impact of the surface states at the YSZ/Si interfaces in the MOS stacks.

## 4. Conclusion

In the present work, we studied the ion migration polarization in the MOM and MOS stacks utilizing the YSZ films deposited by Magnetron Sputtering as the gate insulators. The values of the activation energy for the oxygen ion polarization

Table 1: The parameters of the oxygen ion transport in the YSZ films in the MOM and MOS stacks determined by various methods.

| Substrate | Sublayer material | $d_s$, nm | $d$, nm | $E_a$, eV | | | | $N_l$, $cm^{-3}$ (500 K) | | |
|---|---|---|---|---|---|---|---|---|---|---|
| | | | | *CV* | *IV* | TD | QC | *CV* | *IV* | TD |
| TiN/Ti | Zr | 3 | 10 | — | — | — | 0.53 | — | — | — |
| TiN | –//– | –//– | 40 | — | 0.55 | 0.55 | 0.53 | — | $2.7 \cdot 10^{19}$ | $2.6 \cdot 10^{19}$ |
| –//– | –//– | 8 | 40 | — | 0.56 | 0.46 | — | — | $2.5 \cdot 10^{19}$ | $9.4 \cdot 10^{19}$ |
| TiN/Ti | Ta | 8 | 15 | — | 0.55 | — | — | — | $5.0 \cdot 10^{19}$ | — |
| TiN/Ti | Zr | 3 | 40 | — | 0.59 | — | — | — | $4.3 \cdot 10^{19}$ | — |
| *n*-Si | –//– | –//– | –//– | 0.50 | — | — | — | $5.0 \cdot 10^{17}$* | — | — |
| –//– | Ta | –//– | –//– | 0.29 | 0.30 | — | — | $3.0 \cdot 10^{17}$* | $2.6 \cdot 10^{19}$ | — |
| *p*-Si | Zr | –//– | –//– | 0.50 | — | 0.53 | — | $5.0 \cdot 10^{17}$* | $1.4 \cdot 10^{19}$ | — |

Measuring method: *CV*—*C-V* measurements of the MIS stacks, *IV*—dynamic *I-V* curves, TD—thermal depolarization, QC—quasistatic capacitance. *An underestimate value (see the details in the text).

in YSZ were measured using several different methods. The measurements of the dynamic *I-V* curves, of the depolarization current, and of the quasistatic capacitance of the MOM stacks gave close values of the activation energy (≈0.5 eV) regardless to the materials of the gates (Au/Zr, Au/Ta) and substrates (TiN/Ti, TiN) as well as to the thickness of the YSZ films (ranging from 10 to 40 nm). This result evidences the absence of the discharging of the ions at the electrodes and of the diffusion mechanism of the oxygen ion transport in YSZ. Also, the values of the mobile ion concentration and mobility in the YSZ films were determined for the temperature range 300–510 K. The data on the oxygen ion transport parameters in the YSZ films deposited by Magnetron Sputtering can be useful in modeling the processes of forming and resistive switching in the memristor devices based on the YSZ films, wherein the formation of the conductive filaments goes through the arrangement of the oxygen vacancies in the electric field between the electrodes.

Also, it was found that the *C-V* measurements of the MOS stacks with relatively high density of the surface states at the YSZ/Si interface gave the underestimated values of the mobile oxygen ion concentration. The origin of the underestimate was related to the impact of the surface states at the YSZ/Si interface. Namely, the anomalous hysteresis in the *C-V* and *G-V* curves of the MOS stacks related to the ion migration polarization of YSZ was compensated by the normal hysteresis originating from to the trapping of the electrons or holes onto the surface states.

## Conflicts of Interest

The authors declare that there are no conflicts of interest regarding the publication of this paper.

## Acknowledgments

The authors gratefully acknowledge the financial support from Ministry of Education and Science, Russian Federation (Project no. RFMEFI58717X0042).

## References

[1] D. Ielmini and R. Waser, *Resistive Switching: From Fundamentals of Nanoionic Redox Processes to Memristive Device Applications*, Wiley-VCH Verlag GmbH & Co. KGaA, Weinheim, Germany, 2016.

[2] D. B. Strukov, G. S. Snider, D. R. Stewart, and R. S. Williams, "The missing memristor found," *Nature*, vol. 453, pp. 80–83, 2008.

[3] R. Waser, "Resistive non-volatile memory devices (Invited Paper)," *Microelectronic Engineering*, vol. 86, no. 7-9, pp. 1925–1928, 2009.

[4] D. S. Jeong, R. Thomas, R. S. Katiyar et al., "Emerging memories: resistive switching mechanisms and current status," *Reports on Progress in Physics*, vol. 75, no. 7, Article ID 076502, 2012.

[5] C. Dias, J. Ventura, and P. Aguiar, "Memristive-based neuromorphic applications and associative memories," *Studies in Computational Intelligence*, vol. 701, pp. 305–342, 2017.

[6] L. Spaanenburg and W. J. Jansen, "Networked neural systems," in *CHIPS 2020 VOL. 2: New Vistas in Nanoelectronics*, B. Höfflinger, Ed., pp. 231–242, Springer, Switzerland, 2016.

[7] A. Adamatzky and L. Chua, *Memristor Networks*, Springer International Publishing, London, UK, 2014.

[8] D. Ielmini, "Modeling the universal set/reset characteristics of bipolar RRAM by field- and temperature-driven filament growth," *IEEE Transactions on Electron Devices*, vol. 58, no. 12, pp. 4309–4317, 2011.

[9] R. Waser, R. Dittmann, C. Staikov, and K. Szot, "Redox-based resistive switching memories nanoionic mechanisms, prospects, and challenges," *Advanced Materials*, vol. 21, no. 25-26, pp. 2632–2663, 2009.

[10] O. N. Gorshkov, I. N. Antonov, A. I. Belov, A. P. Kasatkin, and A. N. Mikhaylov, "Resistive switching in metal-insulator-metal structures based on germanium oxide and stabilized zirconia," *Technical Physics Letters*, vol. 40, no. 2, pp. 101–103, 2014.

[11] A. N. Mikhaylov, E. G. Gryaznov, A. I. Belov et al., "Field- and irradiation-induced phenomena in memristive nanomaterials," *Physica Status Solidi (c)—Current Topics in Solid State Physics*, vol. 13, no. 10-12, pp. 870–881, 2016.

[12] O. N. Gorshkov, A. N. Mikhaylov, A. P. Kasatkin et al., "Resistive switching in the Au/Zr/$ZrO_2$-$Y_2O3$/TiN/Ti memristive devices

deposited by magnetron sputtering," *Journal of Physics: Conference Series*, vol. 741, no. 1, Article ID 012174, 2016.

[13] D. V. Guseinov, D. I. Tetelbaum, A. N. Mikhaylov et al., "Filamentary model of bipolar resistive switching in capacitor-like memristive nanostructures on the basis of yttria-stabilised zirconia," *International Journal of Nanotechnology*, vol. 14, no. 7-8, pp. 604–617, 2017.

[14] V. G. Zavodinsky, "The mechanism of ionic conductivity in stabilized cubic zirconia," *Physics of the Solid State*, vol. 46, no. 3, pp. 453–457, 2004.

[15] H. A. Abbas, *Stabilized Zirconia for Solid Oxide Fuel Cells or Oxygen Sensors: Characterization of Structural and Electrical Properties of Zirconia Doped with Some Oxides*, LAP Lambert Academic, Saarbrücken, Germany, 2012.

[16] H. Bentarzi, *Transport in Metal-Oxide-Semiconductor Structures: Mobile Ions Effects on the Oxide Properties*, Springer Berlin Heidelberg, Berlin, Germany, 2011.

[17] E. I. Goldman, A. G. Zhdan, and G. V. Chucheva, "The time–of–flight effect and electron–ion reactions at a dielectric–semiconductor contact during thermostimulated ion depolarization in the characteristics of Si–MOS structures," *Microelectronics*, vol. 33, no. 8, pp. 962–968, 1999.

[18] E. R. Nicollian and J. R. Brews, *MOS (Metal–Oxide–Semiconductor) Physics and Technology*, John Willey & Sons, Hoboken, NJ, USA, 1982.

[19] E. H. Snow, A. S. Grove, B. E. Deal, and C. T. Sah, "Ion transport phenomena in insulating films," *Journal of Applied Physics*, vol. 36, no. 5, pp. 1664–1673, 1965.

[20] S. M. Sze, *Physics of Semiconductor Devices*, Wiley-Interscience, Hoboken, NJ, USA, 2nd edition, 1981.

[21] R. I. Merino and V. M. Orera, "Correlation between intrinsic electron traps and electrical conductivity in stabilized zirconia," *Solid State Ionics*, vol. 76, no. 1-2, pp. 97–102, 1995.

[22] S. G. Dmitriev, "The relationship between the measured currents and charges in the sample in the diagnostics of inhomogeneous dielectric films," *Semiconductors*, vol. 43, no. 6, p. 854, 2009.

[23] R. Coelho, *Physics of Dielectrics—for the Engineer*, vol. 1 of *Fundamental Studies in Engineering*, Elsevier, Amsterdam, The Netherlands, 1979.

[24] S. Starschich, S. Menzel, and U. Böttger, "Evidence for oxygen vacancies movement during wake-up in ferroelectric hafnium oxide," *Applied Physics Letters*, vol. 108, no. 3, Article ID 032903, 2016.

[25] V. M. Orera, R. I. Merino, Y. Chen, R. Cases, and P. J. Alonso, "Intrinsic electron and hole defects in stabilized zirconia single crystals," *Physical Review B: Condensed Matter and Materials Physics*, vol. 42, no. 16, pp. 9782–9789, 1990.

[26] K. L. Ngai, J. Santamaria, and C. Leon, "Dynamics of interacting oxygen ions in yttria stabilized zirconia: bulk material and nanometer thin films," *The European Physical Journal B*, vol. 86, no. 1, Article ID 7, 2013.

[27] A. Tarancón, A. Morata, D. Pla et al., "Grain boundary engineering to improve ionic conduction in thin films for micro-SOFCs," *European Chemical Society Transactions*, vol. 69, no. 16, pp. 11–16, 2015.

[28] S. Geller, *Solid Electrolytes*, Springer Berlin Heidelberg, Berlin, Germany, 2013.

[29] G. Pfister and H. Scher, "Dispersive (non-Gaussian) transient transport in disordered solids," *Advances in Physics*, vol. 27, no. 5, pp. 747–798, 1978.

[30] A. V. Churikov, "On the mechanism of ion transport in solidelectrolyte films on lithium," *Technical Physics Letters*, vol. 75, no. 11, pp. 97–104, 2005.